Cellular & Molecular Biology
Cell. Mol. Biol. 2014; 60 (1): 19-25
Published online March 5, 2014 (http://www.cellmolbiol.com)
Received on January 27, 2014, Accepted on February 17, 2014.
doi : 10.14715/cmb/2013.60.1.4

V-ATPase regulates communication between microvascular endothelial cells and metastatic cells

S. R. Sennoune[1], A. Arutunyan[2], C. del Rosario[1], R. Castro-Marin[1], F. Hussain[1,3] and R. Martinez-Zaguilan[1,3]

[1] Department of Cell Physiology & Molecular Biophysics, Texas Tech University Health Sciences Center, Lubbock, TX
[2] Department of Pharmacology & Physiology, George Washington University Medical Center, Washington, DC
[3] Department of Mechanical Engineering, Texas Tech University, Lubbock, TX

Corresponding author: R. Martinez-Zaguilan, Department of Cell Physiology & Molecular Biophysics, Texas Tech University Health Sciences Center, 3601 4th street, Lubbock, TX 79430-6551. Tel : +1-806-743-2562, Fax : +1-806-743-1512, E-mail: Raul.MartinezZaguilan@ttuhsc.edu

Abstract

To metastasize distant organs, tumor cells and endothelial cells lining the blood vessels must crosstalk. The nature of this communication that allows metastatic cells to intravasate and travel through the circulation and to extravasate to colonize different organs is poorly understood. In this study, we evaluated one of the first steps in this process - the proximity and physical interaction of endothelial and metastatic cells. To do this, we developed a cell separator chamber that allows endothelial and metastatic cells to grow side by side. We have shown in our previous studies that V-ATPases at the cell surface (pmV-ATPase) are involved in angiogenesis and metastasis. Therefore, we hypothesized that the physical proximity/interaction between endothelial and metastatic cells expressing pmV-ATPase will increase its activity in both cell types, and such activity in turn will increase pmV-ATPase expression on the membranes of both cell types. To determine pmV-ATPase activity we measured the proton fluxes (J_{H+}) across the cell membrane. Our data indicated that interaction between endothelial and metastatic cells elicited a significant increase of J_{H+} via pmV-ATPase in both cell types. Bafilomycin, a V-ATPase inhibitor, significantly decrease J_{H+}. In contrast, J_{H+} of the non-metastatic cells were not affected by the endothelial cells and vice-versa. Altogether, our data reveal that one of the early consequences of endothelial and metastatic cell interaction is an increase in pmV-ATPase that helps to acidify the extracellular medium and favors protease activity. These data emphasize the significance of the acidic tumor microenvironment enhancing a metastatic and invasive phenotype.

Key words: pH regulation, proton fluxes, cell separator chamber, angiogenesis, metastasis, imaging.

Introduction

A fundamental question in cancer biology has been what makes tumor cells establish in certain tissues and what environment allows/promotes subsequent colonization to distant organs, i.e., metastasis. The complexity and dynamics of biological systems has impaired answering this fundamental question in vivo. Metastasis is a complex process that requires tumor growth and escape into circulation via intravasation and extravasation (1, 2), involving tumor cell migration and invasion through extracellular matrix (3, 4). However, the process of tumor angiogenesis suggests that there is also active growth and invasion of the extracellular medium by endothelial cells (5) - enabling increased nutrient delivery to the tumor and a pathway for their escape into circulation. Our understanding of endothelial and tumor cell interactions and the molecules involved in this earlier event in metastasis are incomplete.

We have shown that highly metastatic human cancer cells express V-ATPase at the cell surface (6-9) which is important for cell invasion - a hallmark of metastasis. Most tumors exhibit an acidic extracellular pH of ca. 6.5 that is not permissive for growth and survival; yet, surprisingly, tumors and endothelial cells survive this acidic environment (10, 11). We hypothesize that the activity of pmV-ATPase allows cells to extrude acid, and maintain an alkaline intracellular pH even in an acidic environment. In addition, we have shown that growth of human breast cancer cells at acidic extracellular pH (pH^{ex}) induces overexpression of pmV-ATPase (7).

We have shown that microvascular - not macrovascular - endothelial cells, express pmV-ATPase (12, 13). Microvascular endothelial cells are angiogenic, whereas macrovascular ones are much less so. We hypothesize that pmV-ATPase provides an acidic extracellular environment optimum for protease activity that could help degrade extracellular matrix and promote angiogenesis. Coronary microvascular endothelial cells in diabetic mice models do not exhibit pmV-ATPase and are poorly angiogenic (13). Diabetic patients have poor circulation that leads to amputation and have poor recovery of collateral blood formation and circulation following a heart attack. Clearly, pmV-ATPase has significance in angiogenesis (8).

Tumor angiogenesis involves a complex interplay between endothelial cells of blood vessels that supply blood to the tumor, and tumor cells that use the vessels to escape into circulation and metastasize to different organs. However, the mechanisms involved in the earlier stages of tumor metastasis are unclear. We hypothesize that interactions between endothelial and tumor cells exhibiting pmV-ATPase will induce promiscuous overexpression of pmV-ATPase in both cell types because of their dynamic acid extrusion that provides a unique extracellular environment. To test this hypothesis we developed a chamber to grow cells in close proximity with each other. Then, proton fluxes via pmV-ATPase were evaluated by ratio ion fluorescence microscopy in tumor and endothelial cells in the border region.

Our data showed that all human prostate metastatic cancer cells (CL1, PC3 and DU145) respond to the pres-

ence of microvascular endothelial cells with a significant increase in proton fluxes (J_{H+}) via pmV-ATPase. In all of these cases, bafilomycin, an inhibitor of V-ATPase decreased J_{H+}. In contrast, microvascular endothelial cells did not induce significant increases in J_{H+} in non-metastatic cells (LNCaP) or vice-versa.

Materials and methods

Cells

The prostate cancer tumor cell lines LNCaP, CL1 DU145 and PC3 were used in this study. LNCaP cells are androgen-sensitive and poorly tumorigenic. All other cell types are highly tumorigenic, and exhibit invasive and metastatic phenotypes. CL1 was derived from LNCaP by growing the cells depleted from androgen in the medium (30). Androgen deprivation treatment of LNCaP cells was carried out by replacing FBS by charcoal-stripped serum. CL1 has been continually maintained in androgen-depleted medium. LNCaP cells were grown in RPMI 1640 media (Cellgro, Mediatech Inc., VA) supplemented with 10% FBS and antibiotics. DU145 and PC3 cells were also grown in RPMI 1640 media, as LNCaP. The CL1 cells were grown in the same medium as their parental cells except that CL1 medium is supplemented with 5% charcoal-treated serum. The microvascular endothelial cells were grown with RMPI 1640 media supplemented with 10% FBS. These cells were maintained at 5% CO_2 at 37°C.

Cell growth in cell separator chamber

The bottom part of a disposable petri dish (35 mm diameter), was used for plating cells (Figure 1). The top part of a 35 mm petri dish was used to assemble the cell separator. A 25 mm diameter hole was cut on the top part of the petri dish. 2 posts (15 mm x 10 mm x 2 mm) were attached and glued to each side of the hole as shown in bottom of Figure 1. The cell separator chamber made of a rectangular acetate plastic sheet (25 mm x 10 mm x 0.3 mm) touches the bottom part of the petri dish containing a 25 mm diameter coverslip #1 and is covered on both sides using parafilm (folded around the cell separator chamber). The edges on the parafilm on the top are attached to each other by gentle pressure using a surgical straight Kelly forcep (hemostat). The complete assembly is sterilized by UV exposure under the sterile hood overnight. Then, cells (1 x 10^3 from each cell type, i.e., endothelial cells (EC) on one side and tumor cells (TC) (either DU145, PC3, CL1 or LNCaP) on the opposite side are seeded from the top of the petri dish (hole) using a pipetman (10-200 µl) from each side of the cell separator. To maintain the liquid in each chamber of the separator, a stainless steel rod (30 mm diameter x 10 mm width with a 25 mm hole) weighting 50 grams is placed on the top of the petri dish. The weight is needed to allow the parafilm surrounding the separator chamber to attach to the coverslip and effectively separate the media and cells. The complete assembly, containing cells, is placed in the CO_2 incubator and cells are allowed to grow until they spread on each side of the assembly (typically 48 hrs). Then, the top part of the petri dish is carefully lifted and the two cell types are clearly separated by 300 µm gap. Cells move to close the gap and interact with each other after 12-18 hrs, depending on the cell type.

Cytosolic pH measurements

Coverslips with EC and TC were loaded with SNARF-1 (5-[and-6] carboxy-SNARF-1) (Life Science Molecular Probes, Eugene, OR) to measure cytosolic pH and determine H^+ fluxes (J_{H+}) as described previously (7, 31). Loading of fluoroprobe with the membrane permeant acetoxy methyl (AM) ester form of SNARF-1 was performed by incubating cells with 7 µM SNARF-1-AM for 30 min at 37°C in Cell Superfusion Buffer (CSB). The CSB contained the following: 1.3 mM $CaCl_2$, 1 mM $MgSO_4$, 5.4 mM KCl, 0.44 mM KH_2PO_4, 110 mM NaCl, 0.35 mM NaH_2PO_4, 5 mM glucose, 2 mM glutamine, and 20 mM HEPES at pH^{ex} 7.4. Cells were washed and incubated with CSB for additional 30 min at 37°C to wash out non-hydrolyzed dye. Cover slips with cells were placed into a thermostated chamber (PDMI-2, Medical Systems Corp. Greenvale, N.Y), and then fastened onto the stage of a fluorescence inverted microscope (Olympus IX-70). Fluorescence was monitored using a cell imaging system consisting

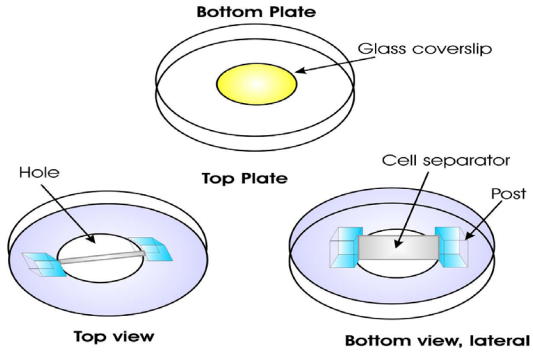

Figure 1. Cell separator chamber device schematic representation. The bottom part of a disposable petri dish (35 mm diameter), was used for plating the cells. The top part of a 35 mm petri dish was used to assemble the cell separator. A 25 mm diameter hole was cut on the top part of the petri dish. 2 posts (15 mm x 10mm x 2 mm) were attached and glued to each side of the hole as shown in Top view Figure. The cell separator was made of a rectangular acetate plastic sheet (25 mm x 10 mm x 0.3 mm). When assembled, the cell separator touches the bottom part of the petri dish containing a 25 mm diameter coverslip #1. The cell separator is covered on both sides using parafilm (folded around the cell separator). The edges on the parafilm on the top are attached to each other by gentle pressure using a straight hemostat tweezer. The complete assemble is sterilized by UV exposure under the sterile hood overnight. Then, cells (10^3 from each cell type, i.e., endothelial cells in one side and tumor cells in the opposite side) are seeded from the top of the petri dish (hole) using a pipetman (10-200 µl) from each side of the cell separator chamber. To maintain the liquid in each chamber of the cell separator, a stainless steel rod (30 mm diameter x 10 mm width with a 25 mm hole) weighting 50 grams is placed on the top of the petri dish. The weight is needed to allow the parafilm surrounding the cell separator to attach to the coverslip and effectively separate media. The complete assembly, containing cells, is placed in the CO2 incubator and cells are allowed to grow until all attached and spread on each side of the assembly (typically 48 hrs). Then, the top part of the petri dish is carefully lifted and the two cell types are clearly separated by 300 µm gap. Cells move to close the gap and interact with each other after 12-18 hrs, depending on the cell type.

of a high speed filter changer (Lambda DG4; Sutter Instruments Co, Novato, CA) to rapidly change excitation filters (484 nm and 534 nm); and a liquid guided optic fiber to deliver the light. The excitation light was reflected using a dichroic mirror (600 DRLPXR). The emission fluorescence of SNARF-1 at 644 nm was obtained by ratio excitation of 488 nm and 534 nm. The fluorescence signal was collected using a frame transfer charged coupled device (CCD) camera coupled to an intensifier (Princeton Instruments Intensifier Pentamax, ADC 5 MHZ). Cells were imaged with an inverted microscope (Olympus IX-70) using a 60x immersion oil objective (1.4 N.A.). In this imaging system, the excitation filters can be changed as fast as 1.5 msec. For these experiments, we used 100 msec exposure. Images were collected and analyzed using Meta Imaging Systems software (Version 4.5; Universal Imaging Corporation, West Chester, PA). Cells were continuously perfused at 3.0 ml/min at 37°C with CSB. After steady-state was reached (5 min), the perfusate was replaced by one containing 50 mM K^+Acetate in a Na^+-free buffer, where Na^+ was substituted with 60 mM N-methylglucamine. The conversion of ratio values to pH^{cyt} was performed as described previously (7, 12). The proton fluxes (J_{H+}) were estimated within the first 3 min of the cytosolic acidification.

Statistical Analysis

All results are expressed as mean ± SEM. Significant differences were determined by using a t-test or an ANOVA with Holm-Sidak test for multiple comparisons of normal distributions. The Mann-Whitney test or the Kruskal-Wallis one way ANOVA on ranks test for multiple comparisons was used for nonparametric distributions (SigmaStat v.3.5; Statistical Software, Jandel Scientific). All statistical tests were considered significant at $p < 0.05$.

Results

Endothelial and tumor cell interactions in the cell separator chamber

The efficacy of the cell separator chamber to grow cells in close proximity is shown in Figure 2. Cells were imaged using an inverted microscope (Olympus IX70) under phase contrast (60x oil objective, 1.4 N.A). Notice that after removal of the cell separator (c.f., Fig 1) there is an apparent cell gap of ~300 µm. The endothelial cells (EC) can be easily distinguished by their birefringence that is higher in the thicker tumor cells (TC) than in the thinner endothelial cells. Notice that at ca.18 hrs, endothelial cells adopt their typical cobblestone morphology. These types of cell cultures were used for pH measurements from individual cells adjacent to the border region, where EC meet with TC. In all the cases, the ECs were clearly differentiated from the TC.

Interaction between TC and EC expressing pmV-ATPase enhances proton fluxes in both cell types

To test the hypothesis that cell-cell interaction increases proton fluxes (J_{H+}) via pmV-ATPases in endothelial and metastatic cells that already expressed pmV-ATPases, we grew cells in a cell separator device and evaluated their ability to extrude acid in response to acid loads. Most cells use the ubiquitous Na^+/H^+ exchanger and HCO_3^--based H^+-transport mechanisms. To eliminate these transporters, we performed acid loading in the absence of Na^+ and HCO_3^-. Under these conditions, only cells that exhibit an alternative cytosolic pH (pH_{cyt}) regulatory mechanism, e.g., pmV-ATPases, will recover from this acidification (7, 12). Figure 3 shows that microvascular endothelial cells (EC) and metastatic prostate cancer cells (CL1) when grown alone, recover from this acid load. In these experiments, cells were intracellularly loaded with SNARF-1, a pH fluorescent indica-

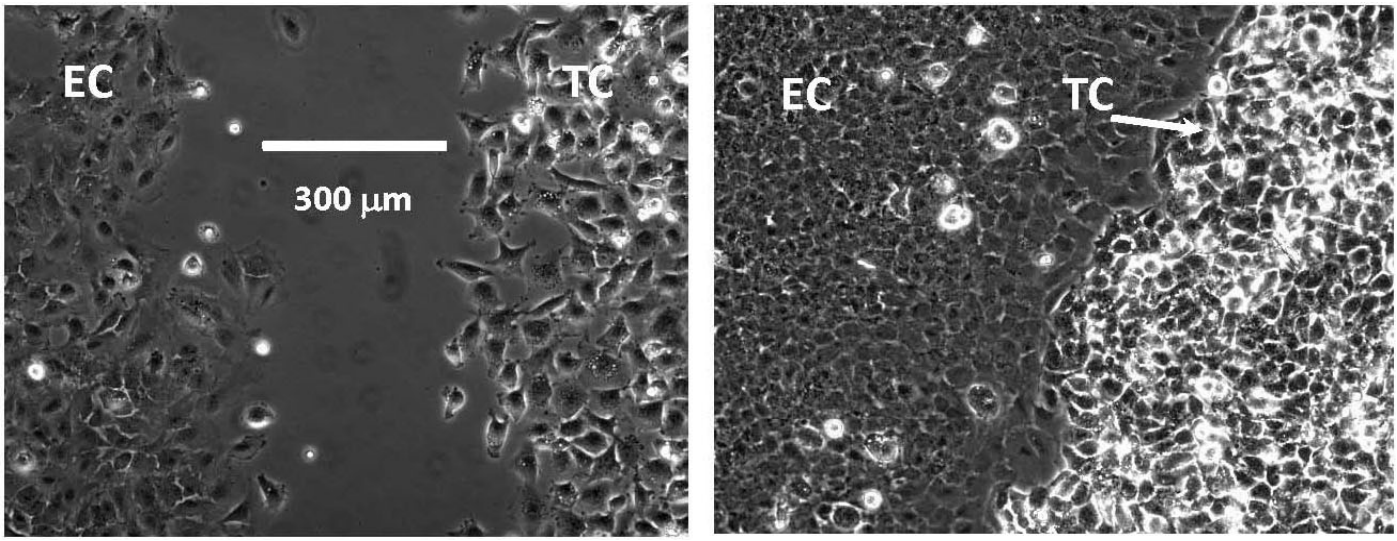

Figure 2. Endothelial and tumor cell interactions in the cell separator chamber. Endothelial (10^3) and tumor (10^3) cells were plated onto a 25 mm glass coverslip, in the cell separator devise, as described in Figure 1. After 48 hrs in culture, the top part of the cell separator was removed leaving a ca. 300 µm gap (Fig 2A). Cells close the gap within 12-18 hrs (Fig 2B). These cells were then intracellularly loaded with SNARF-1, a ratiometric pH fluorescent indicator, by incubating for 30 min at 37°C with the acetoxymethyl ester form of the probe (permeant). Cellular esterases cleave the diester bond and leave the charged form inside of the cell. Then, cells were washed and further incubated for 30 min to remove fluoroprobe that has leaked out of the cell or uncleaved fluoroprobe. The coverslips were then transferred to a cell chamber (25 mm) that was maintained at 37°C using a thermostated apparatus. Cells were imaged using an inverted microscope (Olympus IX70) under phase contrast (60x oil objective, 1.4 N.A.). Notice that endothelial cells (EC) have a cobblestone structure and are thinner than the tumor cells (TC) that at confluence exhibited higher bi-refrigency and makes it easier to identify them. The interaction (border) between cells is conspicuously shown in B.

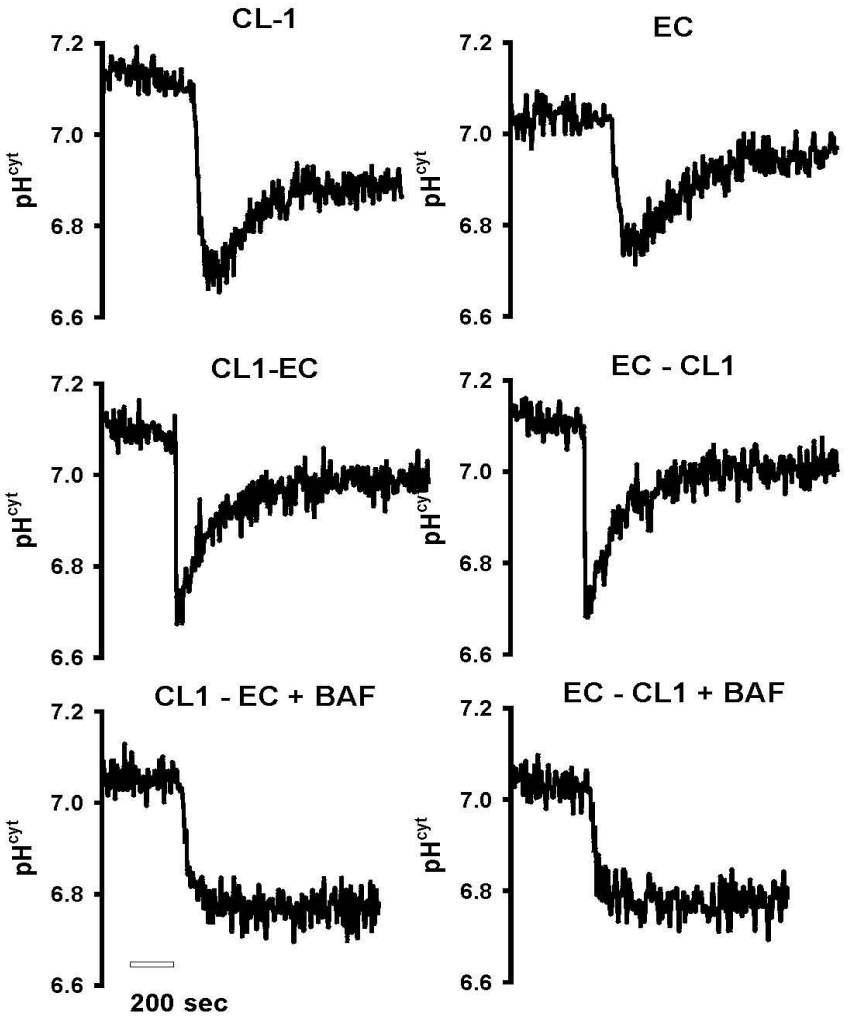

Figure 3. Interaction between tumor cells and endothelial cells increases the rate of recovery (J_{H+}) from an acid load. Cells were intracellularly loaded with SNARF-1, a pH fluorescent indicator. The ion sensitive excitation wavelengths, of SNARF-1, 488 and 534 nm were collected using an emission wavelength of 644 nm (the bandpass of all of these filters is 20 nm). To change filters at millisecond resolution we used the Lambda-DG4 illuminator. We used a liquid guided optical fiber to excite the fluoroprobes on the microscope stage (Olympus IX70, 60x objective oil N.A. 1.4). We used a Cooled Charge-coupled Device (CCD; Pentamax with image intensifier) to collect the fluorescence signal derived from cells loaded with SNARF-1 (100 msec exposure; 3 seconds interval). Cells were superfused at 37°C with buffer during 5 min to obtain steady-state, then the perfusate was exchanged for one containing potassium acetate (50 mM) that elicits a rapid acidification. In these experiments, the buffer does not contain Na^+ or HCO_3^- to eliminate the contribution of the ubiquitous Na^+/H^+ exchanger and HCO_3^- -based H^+- transporting mechanisms. Thus, only cells that exhibit vacuolar type H^+-ATPases at their plasma membrane (pm-V-ATPases) should recover from this acidosis. For purposes of data presentation, only one trace per cell corresponding to either endothelial cell alone (EC), tumor cell alone (CL1); or CL1 interacting with EC on the border region (CL1-EC) and EC interacting with CL1 (CL1-EC) are shown. Data are representative of 3-9 experiments. In each experiment we obtained pH^{cyt} recoveries from 30-50 cells from EC and TC. Notice that the recovery from acid load is faster in tumor cells (CL1) interacting with endothelial cells (EC) than in controls (tumor cells not interacting with endothelial cells). Similarly, pH^{cyt} recoveries are faster in EC cells interacting with CL1 than in control (EC not interacting with tumor cells, top panel). The bottom panels show that bafilomycin decreases the pH^{cyt} recoveries.

tor. After steady state was reached (typically 5-10 minutes), the superfusate was exchanged for one containing potassium acetate that elicits a rapid cytosolic acidification. Notice that both microvascular endothelial cells (EC) and metastatic prostate cancer cells (CL1) recover from this acid load by extruding acid leading to pH^{cyt} recovery towards baseline. Similar data resulted from other metastatic cells used in this study. Only one representative trace of EC and CL1 are presented. Because we evaluated the pH^{cyt} recoveries of individual cells located at the border region, we quantified the pH^{cyt} recoveries of all the EC and TC in the border region (typically 30-50 of each cell type/experiment). We then grew EC and TC in the cell separator device and noticed that the rate of pH^{cyt} recovery were faster (CL1-EC or EC-CL1; Fig 3, middle panel) than when cells were grown alone (Fig 3, top panel). Treatment or cells with bafilomycin, a V-ATPase inhibitor), decreased the rate of pH^{cyt} recovery (CL1-EC+BAF or EC-CL1+BAF).

The summary of all pH^{cyt} recoveries is shown in figure 4. We obtained the derivative of pH^{cyt} recoveries as a function of time (*dpH/dt*) following the nadir of the acidification during 3 minutes. Then, the buffering capacity determined from the magnitude of the acidification was used to determine J_{H+}. Notice that there was a significant increase in J_{H+} when highly metastatic cells expressing pmV-ATPases were grown in the presence of endothelial cells that also express pmV-ATPases. Simi-

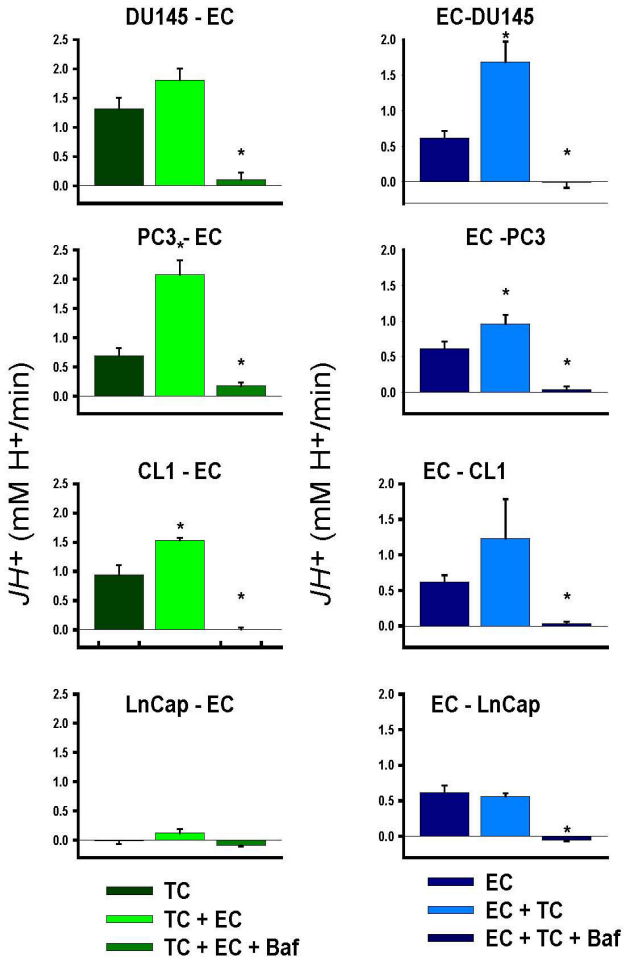

Figure 4. Interaction between tumor and endothelial cells exhibiting pmV-ATPase exacerbates proton fluxes in both cell types. Cells were loaded with SNARF-1 to monitor pH in single cells, as described in Figures 1-3. The rates of proton fluxes (J_{H+}) were estimated during the first 3 minutes following acidification. Notice that highly metastatic human prostate cancer cells DU145, PC3 and CL1 exhibit greater J_{H+} than non-metastatic cells (LNCaP). Interaction with endothelial cells (EC) increases the JH^+ in all cell types, except in non-metastatic LNCaP cells. Bafilomycin, an inhibitor of V-ATPase, decreases the J_{H+} in all cell types. The endothelial cells also exhibit pmV-ATPases and recover from acid loads in the absence of Na^+ and HCO_3^-. Importantly, their interaction with highly metastatic tumor cells (TC) increases the J_{H+}. Notice that endothelial cells do not increase J_{H+} when interacting with non-metastatic LNCaP cells. Bafilomycin decreases the J_{H+} in all the EC studies. Data are representative of 3-9 experiments. In each experiment we evaluated J_{H+} from 30-50 cells from EC and TC. Data represents the mean and SEM.

larly, the J_{H+} was also faster in endothelial cells grown in the presence of highly metastatic cells expressing pmV-ATPases. In all the cases, J_{H+} was significantly decreased by bafilomycin, a V-ATPase inhibitor. In contrast, the non-metastatic (LNCaP) cells (that express significantly less pmV-ATPase than highly metastatic cells) did not respond with an increase in J_{H+} when grown in the presence of microvascular endothelial cells expressing pmV-ATPase. Likewise, the J_{H+} in endothelial cells expressing pmV-ATPases was not affected by the presence of non-metastatic cells. Bafilomycin also decreased J_{H+} in endothelial cells. Altogether, our data indicate that cells expressing pmV-ATPase can exacerbate J_{H+} of adjacent cells provided that they also express

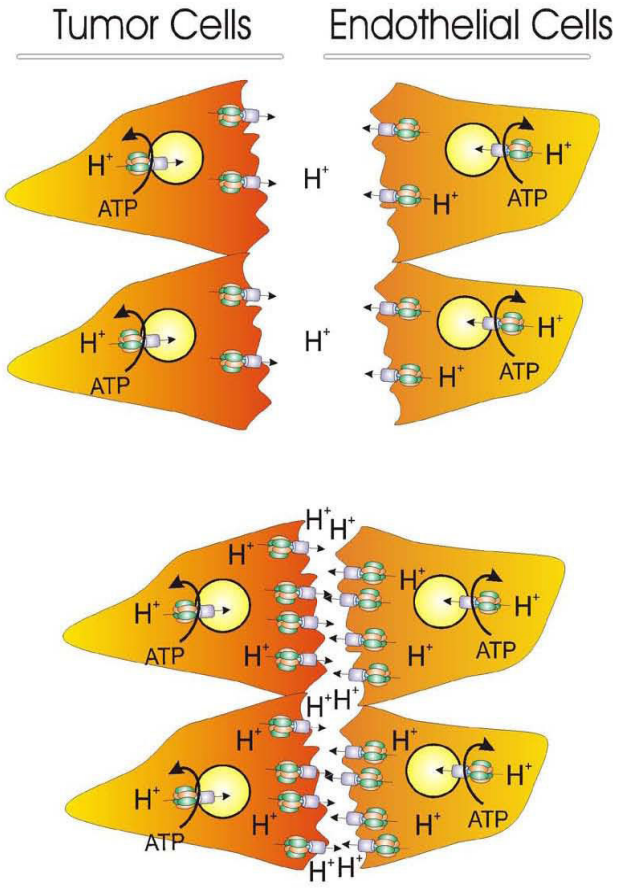

Figure 5. Tumor-endothelial cell interaction induces promiscuous overexpression of VATPases at the plasma membrane (pmV-ATPases). Top, illustrates that when tumor and endothelial cells already expressing pmV-ATPases are distant they maintain their respective levels of pmV-ATPases. When tumor and endothelial cells expressing pmV-ATPase reach close proximity, the local extracellular acid production via pmV-ATPase increases. This triggers increase of pmV-ATPases in both tumor and endothelial cells. When tumor cells exhibit little pmV-ATPase, they do not affect endothelial cells pmV-ATPase.

pmV-ATPase, i.e., promiscuous exacerbation of pmV-ATPase activity.

Discussion

An earlier hypothesis of cancer metastasis indicated that the tumor escapes and travels through circulation to colonize other tissues and organs (1-4). A more recent one, hypothesizes that the tumor induces angiogenesis (5). Further, it has also been suggested that the tumor per se may create a blood vessel like structure to communicate with the blood supply (14, 15). A common denominator in these hypotheses and other variants is the need of either the tumor or the endothelial cells to degrade extracellular matrix; and then migrate and invade through it. There is also a requirement of either mechanical or chemical interaction between endothelial cells lining blood vessels and the tumor. The nature of the signal molecule(s) that leads to the ability of the cell to invade extracellular matrix is unknown. We proposed that acid extrusion via pmV-ATPases is one of the essential signals that prepare the endothelial and metastatic cells to enhance their invasive phenotype.

In this study we have developed a simplified 2D sys-

tem to study cell-cell interaction and the consequences of such interaction, by monitoring cytosolic pH and acid extrusion via pmV-ATPases. We selected well characterized human prostate metastatic cells and microvascular endothelial cells, both exhibiting pmV-ATPase. Our earlier results showed that growth of metastatic cells at acidic extracellular pH enhances their metastatic potential, as seen by increased cell migration and cell invasion through extracellular matrix (7, 10, 16). It is known that the tumor environment is acidic and hypoxic, conditions that are not favorable for cell growth and survival; yet tumor and microvascular endothelial cells thrive in this environment (8, 11, 17, 18). Our data support the hypothesis that pmV-ATPase activity and acidification of the extracellular microenvironment prepare these cells to survive in this environment and enhance their invasive phenotype.

We show that, in agreement with prior studies, all metastatic cells included in this study exhibit pmV-ATPase. This was corroborated using bafilomycin, an inhibitor of V-ATPases. Bafilomycin decreases J_{H+} in highly metastatic and in endothelial cells. Importantly, interaction of endothelial and metastatic cells increased J_{H+} via pmV-ATPase in both cell types. These data suggest that acid extrusion via pmV-ATPase promotes overexpression of pmV-ATPase. Because both endothelial and metastatic cells already exhibit pmV-ATPases, they exacerbate each other's J_{H+}. The non-metastatic cells that exhibit little pmV-ATPase did not affect J_{H+} in endothelial cells. This suggests the acid environment created by pmV-ATPase and not the direct cell-cell interaction responsible for increased overexpression of pmV-ATPase. The lack of response of non-metastatic cells to acid exposure is unclear. We know, however, that pmV-ATPase expression could be due to enhanced exocytosis of vesicles containing V-ATPase and their fusion with the plasma membrane (19, 20). Indeed we have shown that highly metastatic cells exhibit greater calcium oscillations than non-metastatic cells. Decreased calcium dynamics in non-metastatic cells could result in decreased fusiogenic and exocytotic events. There is also the possibility that the non-metastatic cells have less a3 and a4 subunit isoforms that direct V-ATPase to the cell surface. There are four subunit "a" isoforms in V-ATPase (a1, a2, a3, and a4) (16, 21-23). It is known that a1 and a2 isoforms direct V-ATPase to intracellular organelles and vesicles, whereas a3 and a4 isoforms, direct vesicles to the plasma membrane in distinct cell types, including breast cancer cells with enhanced metastatic potential (16). Our unpublished data support the hypothesis that the levels of a3 and a4 isoforms expression, in human non-metastatic prostate cancer cells are lower than in metastatic cells. It is then possible that longer exposure to acidic pH may be needed to change the genotype on those cells lacking the proper "a" subunit isoform(s) that targets V-ATPase to the plasma membrane. This could explain the lack of response of the non-metastatic cells to the presence of endothelial cells. In contrast, metastatic cells that already have pmV-ATPase in the presence of endothelial cells may need only to enhance targeting and recycling of vesicles to the plasma membrane. Further studies to address these issues are needed.

We have shown that V-ATPase preferentially locates to the leading and migratory edge in both endothelial and highly metastatic tumors (7, 12, 13). Here we show that J_{H+} is exacerbated by the acid extrusion in neighboring cells at the border region. We interpret these data to suggest that H^+ work as chemo-attractants and play an important role in cell polarity. Recently, the Wnt/PCP signaling transduction pathway has been shown to be important in cell-cell polarization in stem cell development (24, 25). In these experiments, the cells in close proximity to Wnt ligand exhibit greater responses, as determined by β-catenin activation, than cells distal to Wnt ligand. This creates a morphogenetic ligand that allows for maintenance of pluripotency in regions adjacent to Wnt and a more stable phenotype at distant sites from Wnt. There are recent studies suggesting a role for the V-ATPase, via its subunits, in Wnt signaling pathway (26, 27). One of the accessory proteins of V-ATPase (ATP6ap2) appears to interact with the Wnt pathway (9, 28). In metastatic prostate cancer cells, ATP6ap2 expression is increased (data not shown). ATP6ap2 appears to be not only a chaperone protein needed for V-ATPase assembly, but also works as a proton sensor (29). Altogether, these data indicate that acid extrusion via pmV-ATPase at the leading edge is one of the earlier events leading to cell polarization and organization of a signalosome complex that has significance for tumor angiogenesis and determines a more invasive and metastatic phenotype.

To conclude, we have shown that endothelial and metastatic cells that exhibit pmV-ATPases enhance their pmV-ATPase activity and exacerbate J_{H+} in a positive feedback mechanism, where acid extrusion by endothelial cells enhances acid extrusion by the metastatic cells and vice-versa. This helps us to understand the significance of a tumor acidic environment in the acquisition of a more metastatic and angiogenic phenotype that could be used to develop rational therapies to halt metastasis.

Acknowledgements

We thank Karina Bakunts for technical assistance. Images and data were generated in the Imaging Analysis & Molecular Biology Core Facilities supported by TTUHSC. This work was supported by Cancer Prevention and Research Institute of Texas (CPRIT).

References

1. Chambers, A., Groom, A.C., MacDonald, I.C., Dissemination and growth of cancer cells in metastatic sites, *Nat. Rev. Cancer,* 2002*,* **2**:563-572. doi: 10.1038/nrc865.

2. Klein, C., Parallel progression of primary tumours and metastases, *Nat. Rev. Cancer,* 2009*,* **9**:302-312. doi: 10.1038/nrc2627.

3. Mack, G., Marshall, A., Lost in migration, *Nat. Biotechnol.,* 2010*,* **28**:214-229. doi: 10.1038/nbt0310-214.

4. van Zijil, F., Krupitza, G., Mikulits, W., Initial steps of metastasis: Cell invasion and endothelial transmigration, *Mutat. Res.,* 2011*,* **728**:23-34. doi: 10.1016/j.mrrev.2011.05.002.

5. Folkman, J., Role of angiogenesis in tumor growth and metastasis, *Semin. Oncol.,* 2002*,* **29**:15-18. Doi: 10.1053/sonc.2002.37263.

6. Martínez-Zaguilán, R., Lynch, R.M., Martinez, G.M., Gillies, R.J., Vacuolar-type H(+)-ATPases are functionally expressed in plasma membranes of human tumor cells, *Am. J. Physiol.,*1993,

265:C1015-C1029.
7. Sennoune, S.R., Bakunts, K., Martinez, G.M., Chua-Tuan, J.L., Kebir, Y., Attaya, M.N., Martínez-Zaguilán, R., Vacuolar H^+-ATPase in human breast cancer cells with distinct metastatic potential: distribution and functional activity. *Am. J. Physiol. Cell Physiol.,* 2004*,* **286**:C1443-C1452. doi: 10.1152/ajpcell.00407.2003.
8. Sennoune, S.R., Martínez-Zaguilán, R., Plasmalemmal vacuolar H^+-ATPases in angiogenesis, diabetes and cancer, *J. Bioenerg. Biomembr.,* 2007*,* **39**:427-433. doi: 10.1007/s10863-0079108-8.
9. Sennoune, S.R., Martínez-Zaguilán, R., Vacuolar H(+)-ATPase signaling pathway in cancer, *Curr. Protein Pept. Sci.,* 2012, **13**:152-163. doi: 10.2174/138920312800493197.
10. Martínez-Zaguilán, R., Seftor, E.A., Seftor, R.E., Chu, Y.W., Gillies, R.J., Hendrix, M.J., Acidic pH enhances the invasive behavior of human melanoma cells, *Clin. Exp. Metastasis,* 1996, **14**:176-186. doi: 10.1007/BF00121214.
11. Parks, S., Chiche, J., Pouyssegur, J., pH control mechanisms of tumor survival and growth. *J. Cell Physiol.,* 2011, **226**:299-308. doi: 10.1002/jcp.22400.
12. Rojas, J. D., Sennoune, S.R*.,* Maiti, D., Bakunts, K., Reuveni, M., Sanka, S.C., Martinez, G.M., Seftor, E.A., Meininger, C.J., Wu, G., Wesson, D.E., Hendrix, M.J., Martínez-Zaguilán, R., Vacuolar-type H^+-ATPases at the plasma membrane regulate pH and cell migration in microvascular endothelial cells, *Am. J. Physiol. Heart circulatory Physiol.,* 2006, **291**: H1147-H1157. doi: 10.1152/ajpheart.00166.2006.
13. Rojas, J.D., Sennoune, S.R., Martinez, G.M., Bakunts, K., Meininger, C.J., Wu, G., Wesson, D.E., Seftor, E.A., Hendrix, M.J., Martínez-Zaguilán, R., Plasmalemmal vacuolar H^+-ATPase is decreased in microvascular endothelial cells from a diabetic model. *J. Cell Physiol.,* 2004, **201**:190-200. doi: 10.1002/jcp.20059.
14. Maniotis, A., Folberg, R., Hess, A., Seftor, E.A., Gardner, L.M., Pe'er, J., Trent, J.M., Meltzer, P.S., Hendrix, M.J., Vascular channel formation by human melanoma cells in vivo and in vitro: vasculogenic mimicry, *Am. J. Pathol.,* 1999*,* **155**:739-752. doi: 10.1016/S0002-9440(10)65173-5.
15. Seftor, R., Hess, A.R., Seftor, E.A., Kirschmann, D.A., Hardy, K.M., Margaryan, N.V., Hendrix, M.J., Tumor cell vasculogenic mimicry: from controversy to therapeutic promise, *Am. J. Pathol.,* 2012, **181**:1115-1125. doi:10.1016/j.ajpath.2012.07.013.
16. Hinton, A., Sennoune, S.R., Bond, S., Fang, M., Reuveni, M., Sahagian, G.G., Jay, D., Martinez-Zaguilan, R., Forgac, M., Function of a subunit isoforms of the V-ATPase in pH homeostasis and in vitro invasion of MDA-MB231 human breast cancer cells. *J. Biol. Chem.,* 2009*,* **284**:16400-16408. doi: 10.1074/jbc.M901201200.
17. De Milito, A., Canese, R., Marino, M. L., Borghi, M., Iero, M., Villa, A., Venturi, G., Lozupone, F., Iessi, E., Logozzi, M., Della Mina, P., Santinami, M., Rodolfo, M., Podo, F., Rivoltini, L., Fais, S., pH-dependent antitumor activity of proton pump inhibitors against human melanoma is mediated by inhibition of tumor acidity. *Int. J. Cancer,* 2010*,* **127**:207-219. doi: 10.1002/ijc.25009.
18. Fais, S., De Milito, A., You, H., Qin, W., Targeting vacuolar H^+-ATPases as a new strategy against cancer. *Cancer Res.,* 2007*,* **67**:10627-10630. doi: 10.1158/0008-5472.CAN-07-1805.
19. Marshansky, V., Futai, M., The V-type H(+)-ATPase in vesicular trafficking: targeting, regulation and function. *Curr. Opin. Cell Biol.,* 2008*,* **20**:415-426. doi: 10.1016/j.ceb.2008.03.015.
20. Nanda, A., Brumell, JH, Nordstrom, T, Kjeldsen, L, Sengelov, H, Borregaard, N, Rotstein, OD, Grinstein, S., Activation of proton pumping in human neutrophils occurs by exocytosis of vesicles bearing vacuolar-type H^+-ATPases. *J. Biol. Chem.,* 1996*,* **271**:15963-15970. doi: 10.1074/jbc.271.27.15963.
21. Forgac, M., Vacuolar ATPases: rotary proton pumps in physiology and pathophysiology. *Nat. Rev. Mol. Cell Biol.*, 2007, **8**:917-929. doi: 10.1038/nrm2272.
22. Sun-Wada, G., Wada, Y., Vacuolar-type proton pump ATPases: roles of subunit isoforms in physiology and pathology. *Histol. Histopathol.,* 2010, **25**:1611-1620.
23. Toei, M., Saum, R., Forgac, M., Regulation and isoform function of the V-ATPases, *Biochemistry,* 2010, **49**:4715-4723. doi: 10.1021/bi100397s
24. Cadigan, K., Nusse, R., Wnt signaling: a common theme in animal development, *Genes Dev.,* 1997, **11**:3286-3305. doi: 10.1101/gad.11.24.3286.
25. Katoh, M., WNT/PCP signaling pathway and human cancer, *Oncol. Rep.,* 2005, **14**:1583-1588.
26. Hermle, T., Petzoldt, A.G., Simons, M., The role of proton transporters in epithelial Wnt signaling pathways, *Pediatric nephrology,* 2011*,* **26**:1523-1527. doi: 10.1007/s00467-011-1823-z.
27. Hermle, T., Saltukoglu, D., Grunewald, J., Walz, G., Simons, M., Regulation of Frizzled-dependent planar polarity signaling by a V-ATPase subunit. *Curr. Biol.,* 2010*,* **20**:1269-1276. doi: 10.1016/j.cub.2010.05.057.
28. Cruciat, C.M., Ohkawara, B., Acebron, S. P., Karaulanov, E., Reinhard, C., Ingelfinger, D., Boutros, M., Niehrs, C., Requirement of prorenin receptor and vacuolar H^+-ATPase-mediated acidification for Wnt signaling, *Science,* 2010*,* **327**:459-463. doi: 10.1126/science.1179802.
29. Kinouchi, K., Ichihara, A., Sano, M., Sun-Wada, G.H., Wada, Y., Kurauchi-Mito, A., Bokuda, K., Narita, T., Oshima, Y., Sakoda, M., Tamai, Y., Sato, H., Fukuda, K., Itoh, H., The (Pro)renin receptor/ATP6AP2 is essential for vacuolar H^+ ATPase assembly in murine cardiomyocytes, *Circ. Res.,* 2010*,* **107**:30-34. doi: 10.1161/ CIRCRESAHA.110.224667.
30. Tso, C.L., McBride, W.H., Sun, J., Patel, B., Tsui, K.H., Paik, S.H., Gitlitz, B., Caliliw, R., van Ophoven, A., Wu, L., deKernion, J., Belldegrun, A., Androgen deprivation induces selective outgrowth of aggressive hormone-refractory prostate cancer clones expressing distinct cellular and molecular properties not present in parental androgen-dependent cancer cells, *Cancer journal*, 2000, **6**:220-233.
31. Sanchez-Armass, S., Sennoune, S.R., Maiti, D., Ortega, F., Martinez-Zaguilan, R., Spectral imaging microscopy demonstrates cytoplasmic pH oscillations in glial cells. *Am. J. Physiol. Cell Physiol.,* 2006*,* **290**:C524-538. doi: 10.1152/ajpcell.00290.2005.